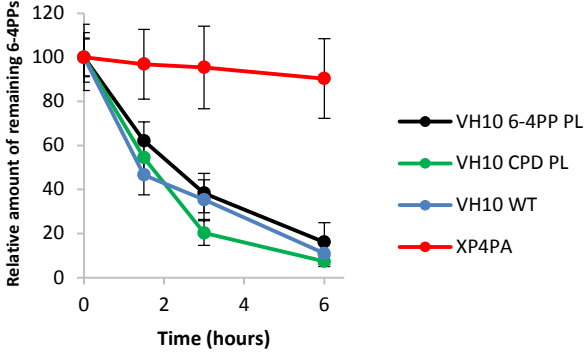
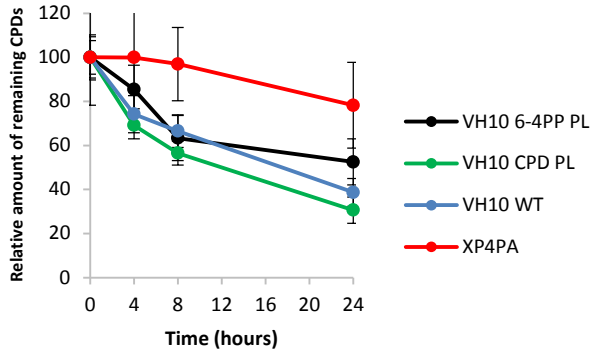


Supplementary Figure S1

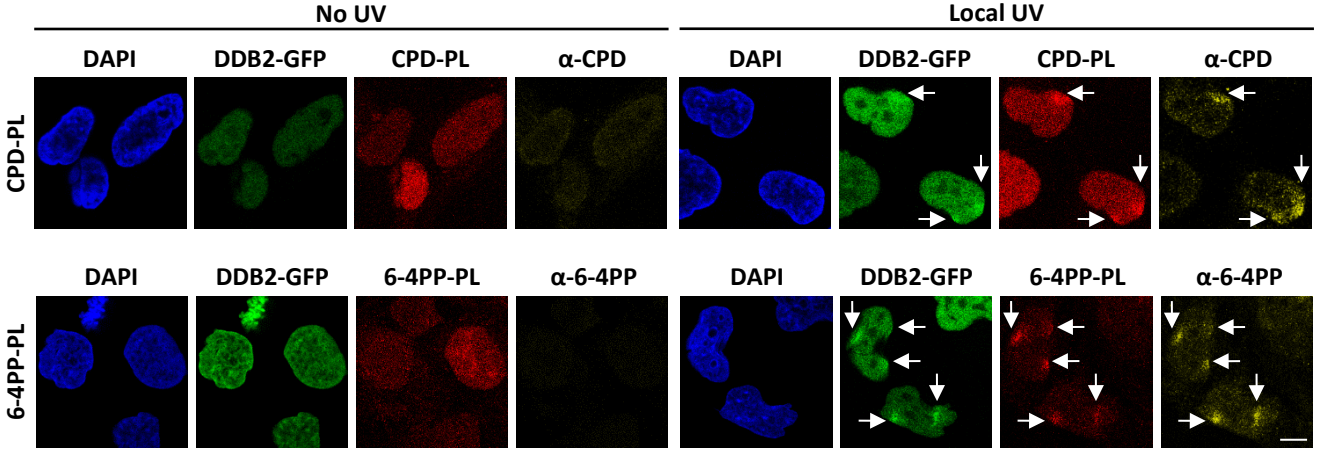
A



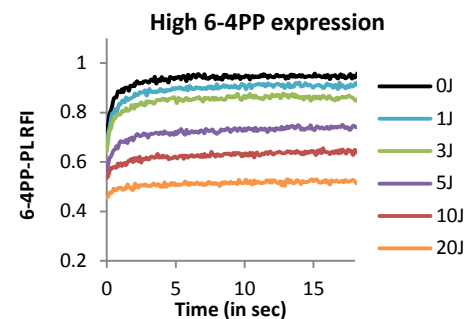
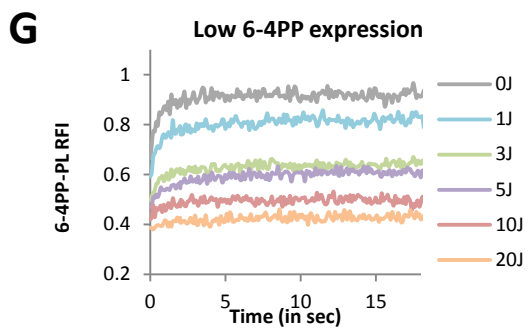
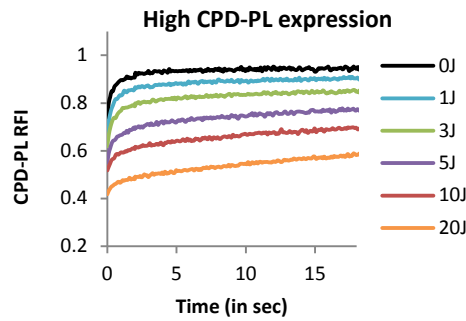
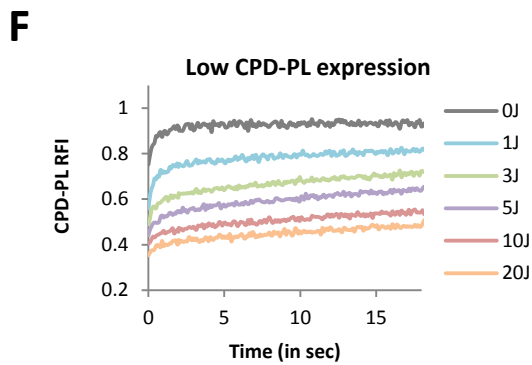
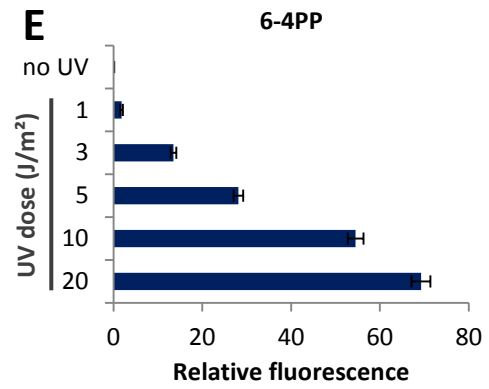
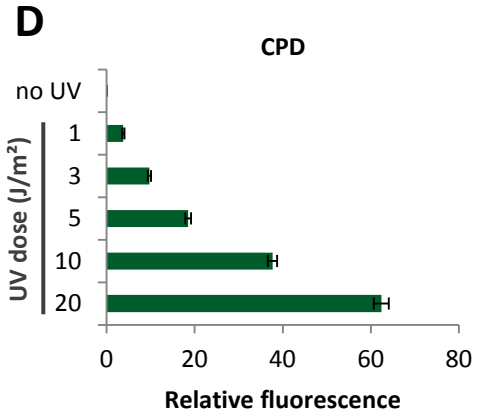
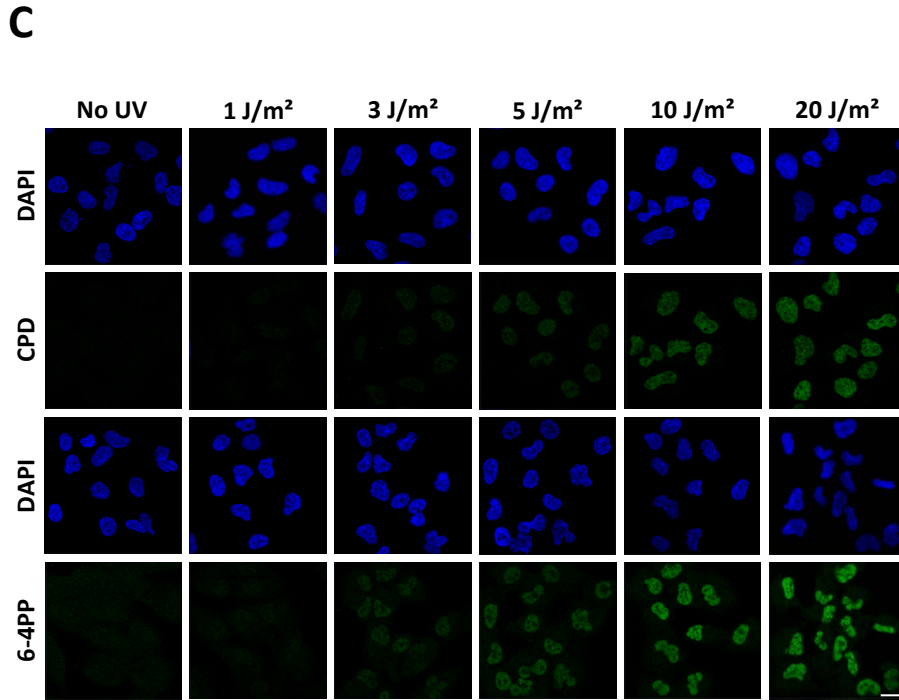
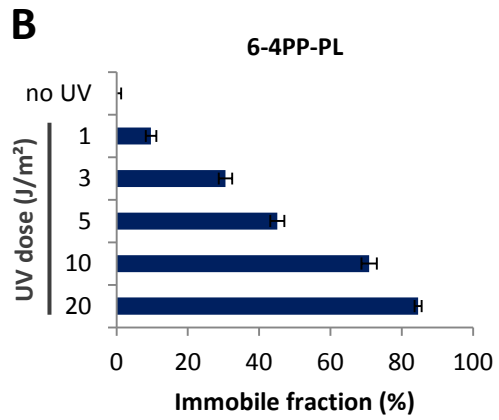
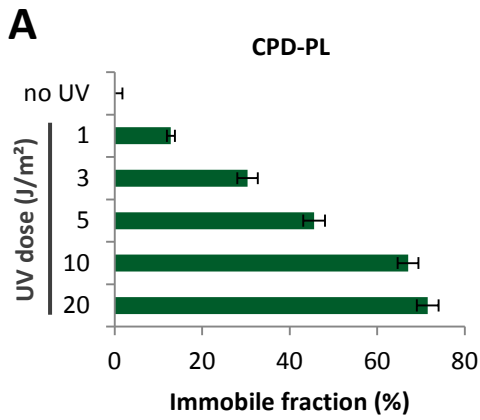
B



C

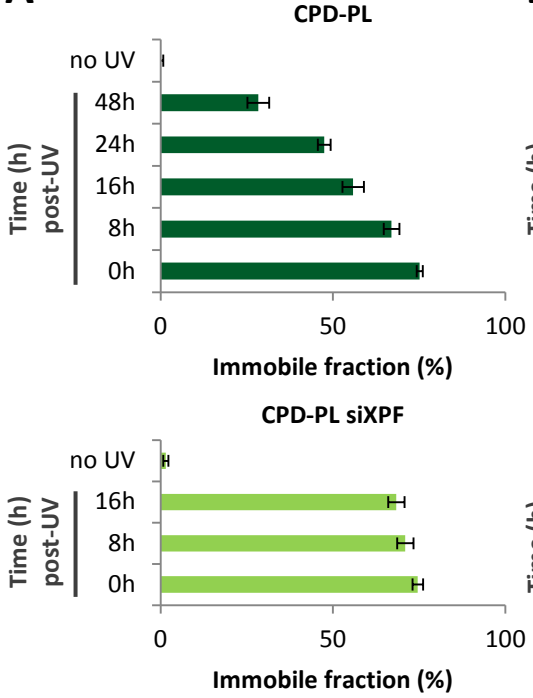


Supplementary Figure S2

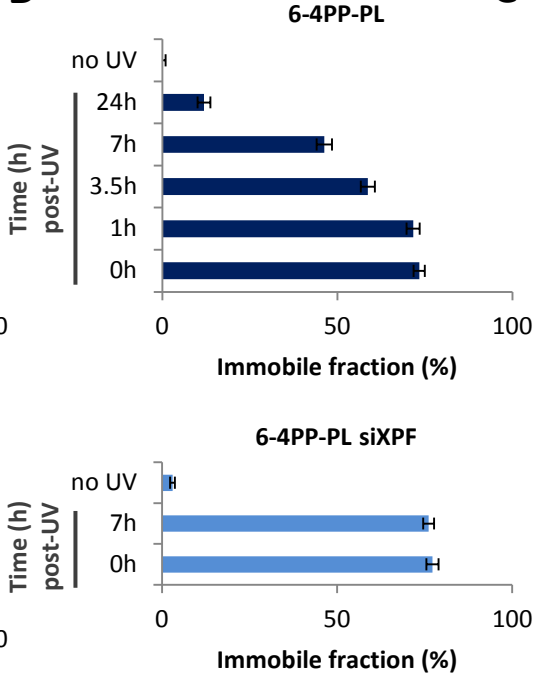


Supplementary Figure S3

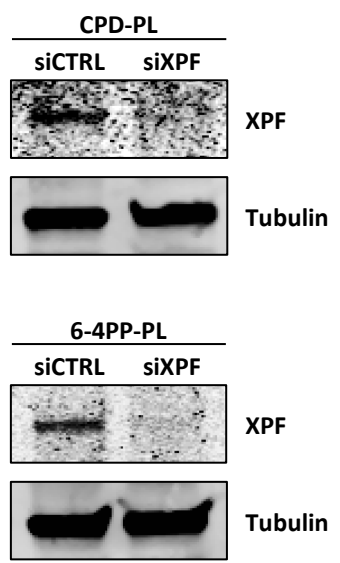
A



B

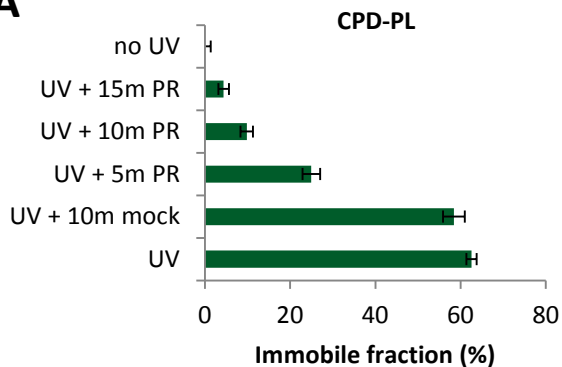


C

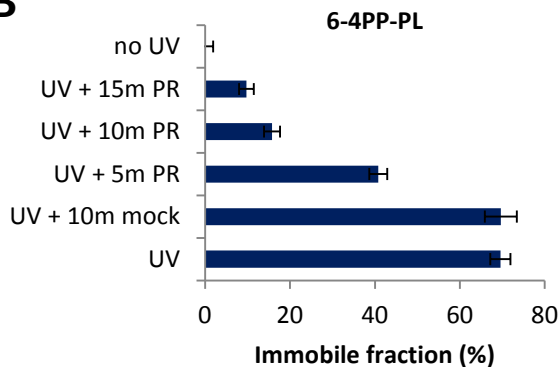


Supplementary Figure S4

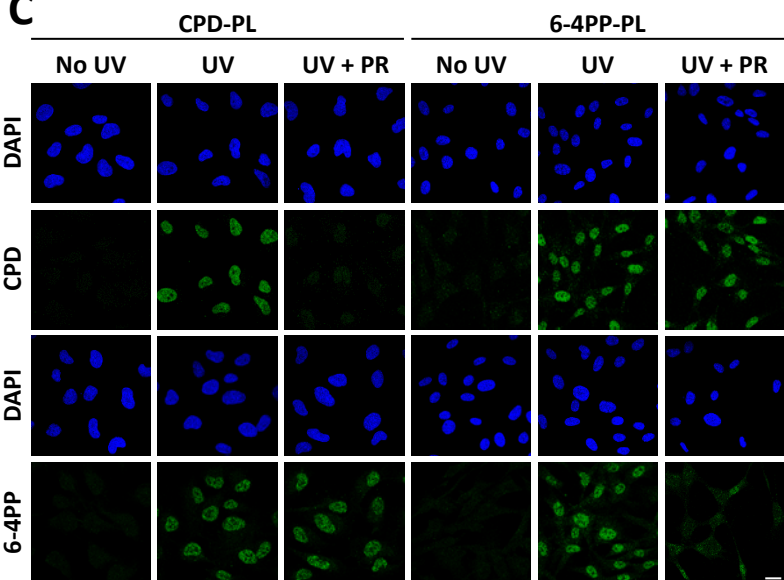
A



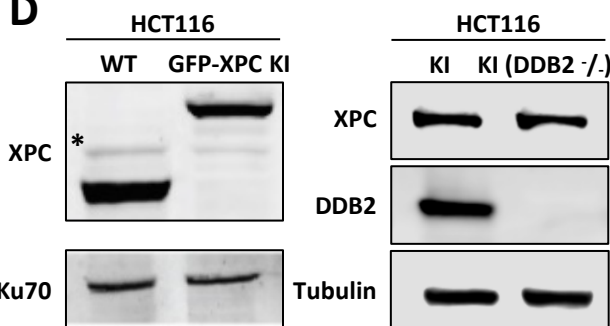
B



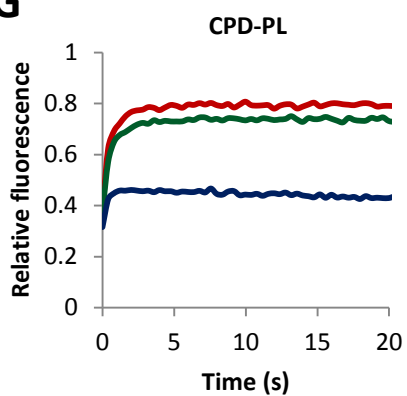
C



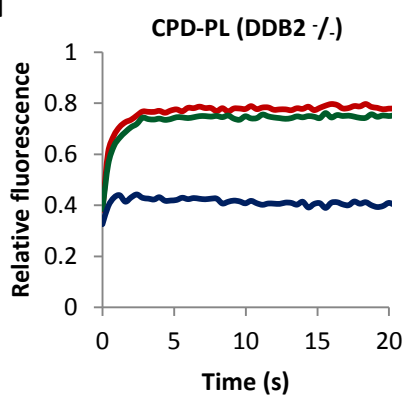
D



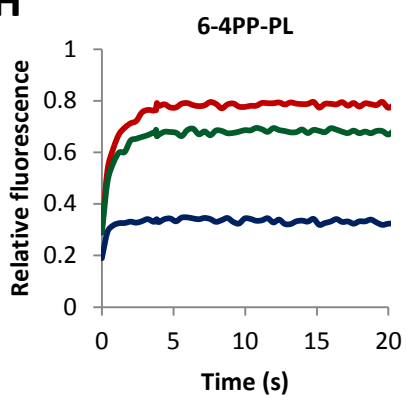
G



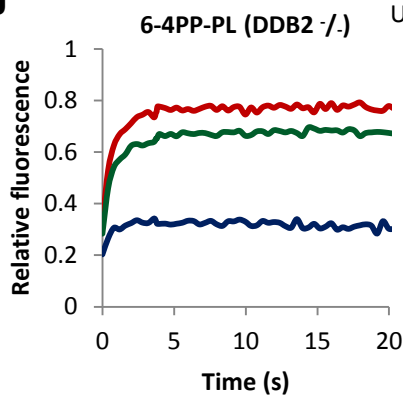
I



H

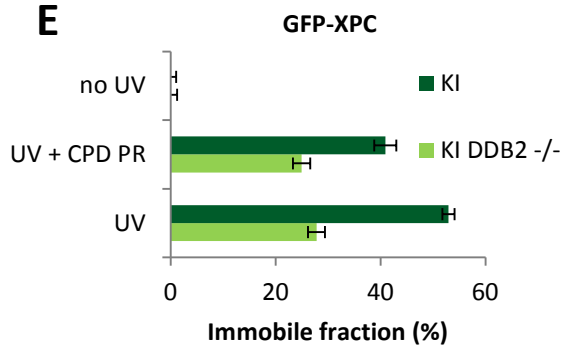


J

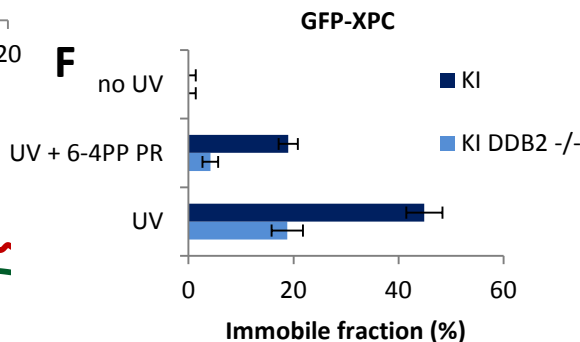


— no UV — UV + PR — UV

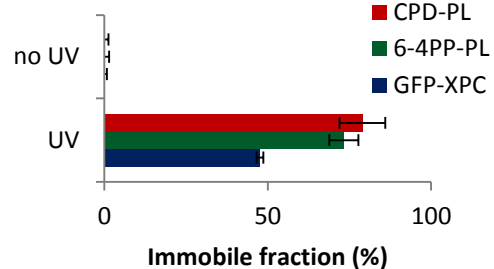
E



F

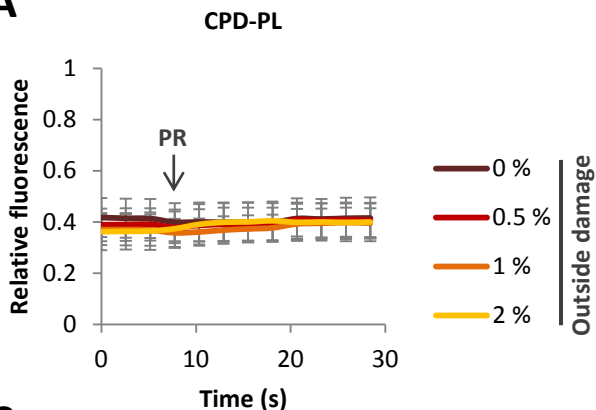


K

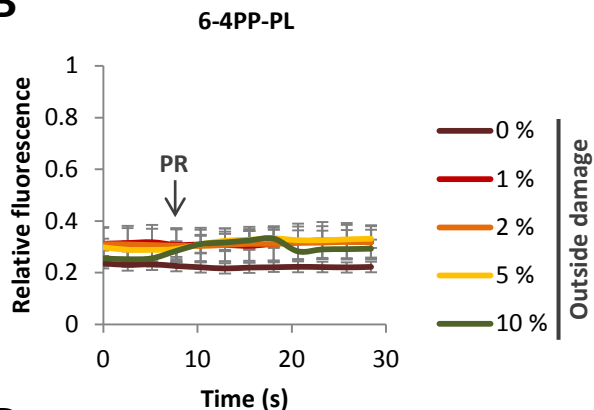


Supplementary Figure S5

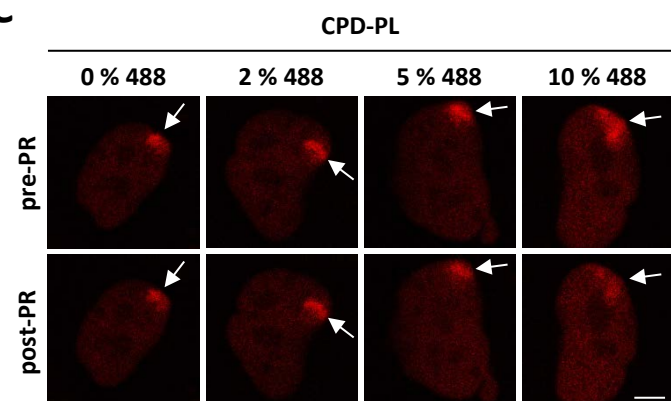
A



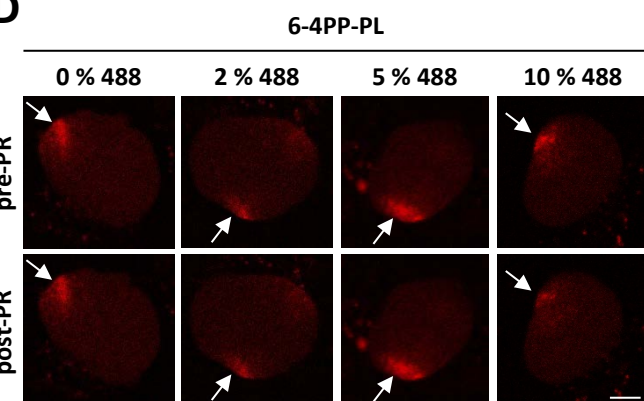
B



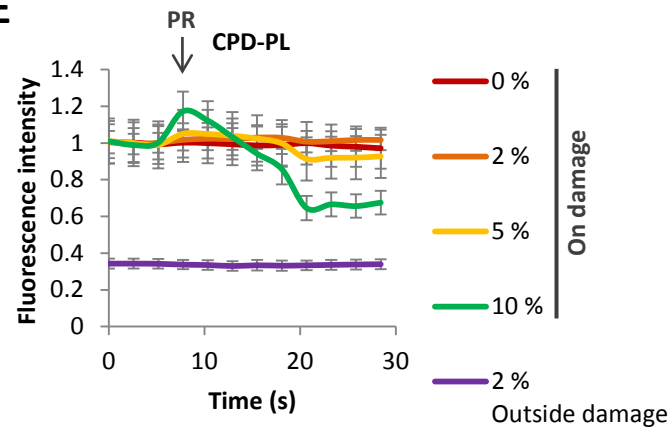
C



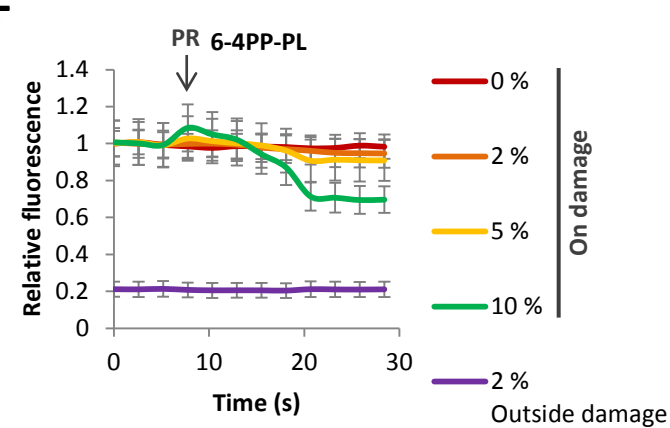
D



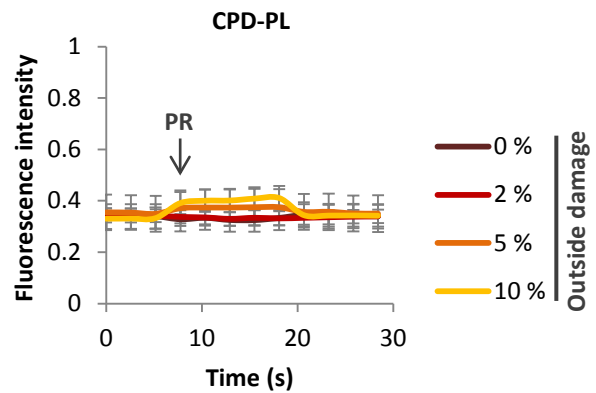
E



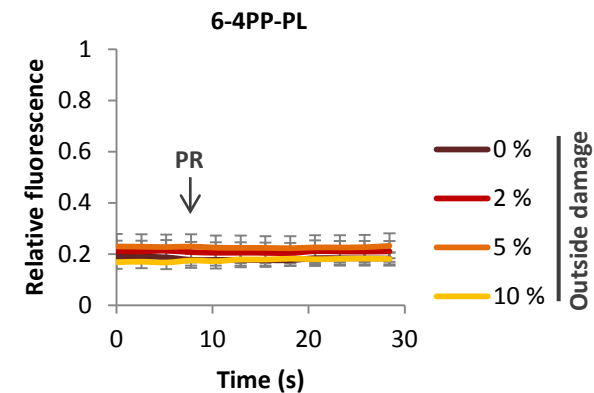
F



G



H



Supplementary Figure Legends:

Supplementary Figure 1.

(A and B) The kinetics of endogenous DNA damage removal by NER was determined by quantifying the levels of 6-4PPs in time after 16 J/m² **(A)** and CPDs in time after 10 J/m² **(B)** by immunofluorescence using 6-4PP and CPD specific antibodies. VH10 wild type cells (WT), VH10 cells expressing CPD-PL or 6-4PP-PL, and NER-compromised (XP-C) XP4PA cells were UV-irradiated and allowed to repair for the indicated time points. Relative fluorescence directly after UV exposure was set at 100% and average fluorescence intensities were plotted in time (n>150 cells of 2 independent experiments +/- SEM). **(C)** Representative immunofluorescence images of GFP-DDB2 expressing VH10 cells that were transduced with either CPD-PL (upper panel) or 6-4PP-PL (lower panel). Cells were non-irradiated or locally UV-C irradiated (60 J/m²), directly fixed and stained with CPD or 6-4PP antibodies as indicated. Arrows indicate local UV damages. Scale bar: 7.5 µm.

Supplementary Figure 2. (A and B) Immobile fractions of CPD-PL **(A)** and 6-4PP-PL **(B)** expressing VH10 cells in non-irradiated or globally UV-C irradiated at the indicated UV doses as determined by FRAP analyses shown in Figure 2A and 2B. Immobile fractions are calculated using the following formula: Immobile fraction (%) = 1 - ((average fluorescence intensity of UV-irradiated cells - the first post-bleach data point) / (average fluorescence intensity of non-irradiated cells - the first post-bleach data point)). The average fluorescence intensities are calculated over the measurements of the last 10 s. (n = 20 cells from 2 independent experiments, mean ± SEM). **(C)** Representative immunofluorescence images of non-irradiated (no UV) or globally UV-irradiated VH10 cells with the indicated UV doses, directly fixed and stained with CPD or 6-4PP antibodies as indicated. Scale bar: 25 µm. **(D)** CPD or **(E)** 6-4PP lesions (Supplementary Figure S3C) were quantified by determining the mean relative fluorescence intensities in immunofluorescence assays using lesion-specific antibodies. (n ≥ 50 cells, mean ± SEM). UV-treated conditions were background corrected by subtracting the mean fluorescence intensity of the non-irradiated condition. **(F and G)** UV dose-dependent immobilization of CPD-PL **(F)** and 6-4PP-PL **(G)** expressing VH10 cells with low (left panel) or high (right panel) PL expression levels. Non-irradiated or globally UV-irradiated cells were analyzed directly after irradiation with the indicated UV doses. Relative fluorescence intensity (RFI) values were normalized to the average pre-bleach signal (n=20 cells from 2 independent experiments).

Supplementary Figure 3. (A and B) Immobile fractions of CPD-PL **(A)** and 6-4PP-PL **(B)** in VH10 cells, which were transfected with control (upper panel) or XPF (lower panel) siRNAs, were determined by FRAP analyses shown in Figure 3E and 3F. (n ≥ 15 cells from 2 independent experiments, mean ± SEM). **(C)** siRNA-mediated XPF knockdown was assessed by immunoblotting VH10 lysates with XPF antibody, tubulin staining was used as loading control.

Supplementary Figure 4. (A and B) Immobile fractions of non-irradiated, globally UV-irradiated (10 J/m²), or globally UV-irradiated (10 J/m²) and photo-reactivated CPD-PL **(A)** and 6-4PP-PL **(B)** as

determined by the FRAP analyses depicted in Figure 3A and 3B. **(C)** Representative immunofluorescence images of CPD-PL or 6-4PP-PL-expressing VH10 cells using 6-4PP or CPD lesion specific antibodies as indicated. Cells were non-irradiated, globally UV-irradiated (10 J/m²), or globally UV-irradiated (10 J/m²) and photo-reactivated (10 min PR), directly fixed and stained using immunofluorescence. Scale bar: 25 μm. **(D)** Upper panel; Expression of the full-length GFP-XPC protein and the concomitant loss of wild type (WT) XPC expression was confirmed by western blotting the lysates from WT and GFP-XPC knock-in HCT116 cell lines with an XPC antibody. Ku70 staining was used as loading control. * indicates an unspecific band. Lower Panel; CRISPR/Cas9-mediated DDB2 knock-out in GFP-XPC HCT116 cells was confirmed by western blotting with a DDB2 antibody. **(E and F)** Immobile fractions of non-irradiated, globally UV-irradiated (10 J/m²), or globally UV-irradiated (10 J/m²) and photo-reactivated (10 min) CPD-PL **(E)** and 6-4PP-PL **(F)** expressing GFP-XPC or GFP-XPC DDB2^{-/-} (DDB2^{-/-}) HCT116 cells determined in the FRAP analyses depicted in Figure 3C-F. **(G and H)** FRAP analyses of PL-mCherry in non-irradiated, globally UV-irradiated (10 J/m²), or globally UV-irradiated (10 J/m²) and photo-reactivated (10 min) CPD-PL **(G)** and 6-4PP-PL **(H)** expressing GFP-XPC HCT116 cells. **(I and J)** FRAP analyses of PL-mCherry in non-irradiated, globally UV-irradiated (10 J/m²), or globally UV-irradiated (10 J/m²) and photo-reactivated (10 min) CPD-PL **(I)** and 6-4PP-PL **(J)** expressing GFP-XPC DDB2^{-/-} HCT116 cells (n ≥ 20 cells from 2 independent experiments, mean ± SEM). **(K)** Direct comparison of immobile fractions of CPD-PL, 6-4PP-PL and GFP-XPC in non-irradiated or globally UV-irradiated (XX J/m²) cells (n ≥ 20 cells from 2 independent experiments, mean ± SEM).

Supplementary Figure 5. (A and B) Relative mCherry fluorescence signal of CPD-PL **(A)** and 6-4PP-PL **(B)** in a non-damaged nuclear region following PR normalized to pre-PR intensities at the local damage (n = 8 cells, mean ± SEM). Cells were locally UV-irradiated (60 J/m²), then a non-damaged nuclear region was exposed after 7.5 sec (indicated by arrow and PR) to the indicated intensities of 405 nm laser for 13 s. (n = 8 cells, mean ± SEM). **(C and D)** Representative images of CPD-PL **(C)** and 6-4PP-PL **(D)** expressing VH10 cells before and 13 s after PR using 488nm laser at the indicated intensity. Arrows indicate local UV damages. Scale bar: 5 μm. **(E, F, G and H)** Cells were locally UV-irradiated (60 J/m²), the local DNA damage spot and a region of the exact same size outside the damage within the nucleus were exposed after 7.5 s (indicated by arrow and PR) to the indicated intensities of 488 nm laser for 13 s. Relative fluorescence signal normalized to pre-PR intensities at the local damage of the mCherry-tagged PLs was quantified inside **(E and F)** and outside **(G and H)** the DNA damage within the nucleus. (n = 8 cells, mean ± SEM).